Kilhoffer, M. C., Demaille, J. C., & Gerard, D. (1981) *Biochemistry 20*, 4407–4414.
Kimura, T., & Ting, J. J. (1971) *Biochem. Biophys. Res. Commun. 45*, 1227–1231.
Kimura, T., Ting, J. J., & Huang, J. J. (1972) *J. Biol. Chem. 247*, 4476–4479.
Klee, C. B. (1977) *Biochemistry 16*, 1017–1024.
Klee, C. B., & Vanaman, T. C. (1982) *Adv. Protein Chem. 35*, 213–321.
Krebs, J., & Carafoli, E. (1982) *Eur. J. Biochem. 124*, 619–624.
Kretsinger, R. H. (1980) *Ann. N.Y. Acad. Sci. 356*, 14–19.
Ikura, M., Hiraoki, T., Hikichi, K., Mikuni, T., Yazawa, M., & Yagi, K. (1983a) *Biochemistry 22*, 2568–2572.
Ikura, M., Hiraoki, T., Hikichi, K., Mikuni, T., Yazawa, M., & Yagi, K. (1983b) *Biochemistry 22*, 2573–2579.
Lim, B. C., & Kimura, T. (1980) *J. Biol. Chem. 255*, 2440–2444.
Longworth, J. W. (1981) *Ann. N.Y. Acad. Sci. 366*, 237–245.
Longworth, J. W., & Rahn, R. O. (1967) *Biochim. Biophys. Acta 147*, 526–535.
Porath, J. (1974) *Methods Enzymol. 34*, 13–20.
Pundak, S., & Roche, R. S. (1983) *Biophys. J. 41*, 220a.
Rayner, D. M., Krajcarski, D. T., & Szabo, A. G. (1978) *Can. J. Chem. 56*, 1238–1245.
Richman, P. G. (1978) *Biochemistry 17*, 3001–3005.
Richman, P. G., & Klee, C. B. (1978) *Biochemistry 17*, 928–935.
Richman, P. G., & Klee, C. B. (1979) *J. Biol. Chem. 254*, 5372–5376.
Sasagawa, T., Ericsson, L. W., Walsh, K. A., Schreiber, W. E., Fisher, E. H., & Titani, K. (1982) *Biochemistry 21*, 2565–2569.
Szabo, A. G., Lynn, K. R., Krajcorski, D. T., & Rayner, D. M. (1978) *FEBS Lett. 94*, 249–252.
Szabo, A. G., Lynn, K. R., Krajcorski, D. T., & Rayner, D. M. (1979) *J. Lumin. 18*, 582–585.
Taylor, D. L., & Fechheimer, M. (1981) in *Calmodulin and Intracellular $Ca^{2+}$ Receptors* (Kakiuchi, S., Hidaka, H., & Means, A. R., Eds.) pp 349–372, Plenum Press, New York.
Vincenzi, F. F., Hinds, T. R., & Raess, B. U. (1980) *Ann. N.Y. Acad. Sci. 356*, 233–244.

# The Rate-Limiting Step in the Actomyosin Adenosinetriphosphatase Cycle†

L. A. Stein,‡ P. B. Chock, and E. Eisenberg*

ABSTRACT: We have previously shown that myosin does not have to detach from actin during each cycle of ATP hydrolysis. In the present study, using the A-1 isoenzyme of myosin subfragment 1, we have investigated the nature of the rate-limiting steps in the ATPase cycle. Our results show that, at 15 °C, at very low ionic strength, $K_{ATPase}$ determined from the double-reciprocal plot of ATPase activity vs. actin concentration is more than 6-fold stronger than $K_{BINDING}$ determined by directly measuring the binding of A-1 myosin subfragment 1 to actin during steady-state ATP hydrolysis. Computer modeling shows that this large difference between $K_{ATPase}$ and $K_{BINDING}$ is not compatible with $P_i$ release being the rate-limiting step in the ATPase cycle. If $P_i$ release is not rate limiting, it is possible that the ATP hydrolysis step, itself, is rate limiting. However, this predicts that, at high actin concentration, the value of the initial $P_i$ burst should be close to zero. Therefore, we measured the magnitude of the initial $P_i$ burst in the presence of actin, using both direct measurement and measurement of relative fluorescence magnitude. Our results suggest that the magnitude of the initial $P_i$ burst in the presence of actin is considerably higher than would be expected if the ATP hydrolysis step were the rate-limiting step in the ATPase cycle. However, we can explain all of our data if there is a special rate-limiting step in the cycle that follows the ATP hydrolysis step, precedes the $P_i$ release step, and occurs at about the same rate whether myosin subfragment 1 is bound to or dissociated from actin. This rate-limiting step may play an important role in determining the velocity of muscle contraction.

It is now generally accepted that muscle contraction is driven by a cyclic interaction of the two muscle proteins, actin and myosin, coupled to the hydrolysis of ATP. Considerable information is now available about the mechanism of the actomyosin ATPase activity in vitro (Adelstein & Eisenberg, 1980). Most of this information has been obtained in steady-state and pre-steady-state kinetic studies with the soluble fragments of myosin, heavy meromyosin (HMM), and subfragment 1 (S-1). However, one major question remains unresolved, the nature of the rate-limiting step in the ATPase cycle. This question is particularly important because, for a wide variety of different muscles, the rate of the actomyosin ATPase activity correlates with the speed of muscle contraction (Barany, 1967).

Until recently, it was assumed that S-1 had to detach from actin during each cycle of ATP hydrolysis (Lymn & Taylor, 1971; Eisenberg & Keilley, 1972); ATP binding was thought to irreversibly dissociate the S-1 from actin, and the ATP hydrolysis step was thought to occur only after S-1 dissociated from actin. However, recent work (Stein et al., 1979, 1981; Mornet et al., 1981) has clearly demonstrated that ATP does

† From the Laboratory of Cell Biology and the Laboratory of Biochemistry, National Heart, Lung, and Blood Institute, National Institutes of Health, Bethesda, Maryland 20205. *Received August 16, 1983.* A preliminary report of this work was presented at the 1982 Biophysics Meeting (Stein et al., 1982).

* Address correspondence to this author at the Laboratory of Cell Biology.
‡ Present address: Department of Cardiology, State University of New York at Stony Brook, Stony Brook, NY 11794.

not irreversibly dissociate S-1 from actin and the ATP hydrolysis step occurs whether S-1 is bound to or dissociated from actin. On this basis, two kinetic models (Schemes I and II), which differ only in the nature of the rate-limiting step, have been proposed to explain the mechanism of the actomyosin ATPase activity (Stein et al., 1979).

Scheme I: Four-State Model[a]

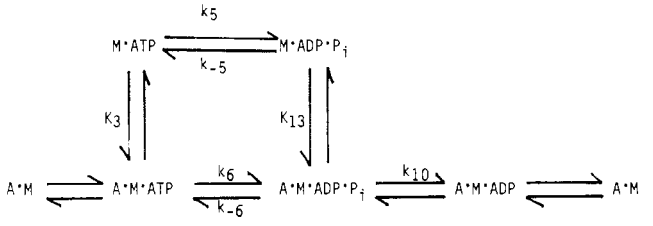


[a] A = actin; M = myosin subfragment 1.

Scheme II: Six-State Model[a]

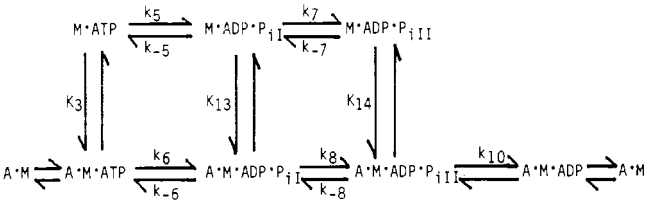


[a] A = actin; M = myosin subfragment 1.

In the four-state model, there are four kinetic intermediates with phosphate in the form of ATP or ADP·$P_i$ bound to the myosin. In the six-state model, there are six kinetic intermediates with phosphate bound. The basic properties of the two models are identical: ATP weakens the binding of S-1 to actin by 4–5 orders of magnitude; hydrolysis of ATP at the active site occurs whether S-1 is bound to or dissociated from actin; M·ATP and M·ADP·$P_i$ bind with nearly equal affinity to actin. The models differ only in the nature of the rate-limiting step. In the four-state model, either the ATP hydrolysis step (A·M·ATP → A·M·ADP·$P_i$), the $P_i$ release step (A·M·ADP·$P_i$ → A·M·ADP), or some combination of the two steps is assumed to be rate limiting. In the six-state model, a specific step has been proposed to be rate limiting, the conformational change from M·ADP·$P_{iI}$ to M·ADP·$P_{iII}$. Like the ATP hydrolysis step, this step is assumed to occur at about the same rate whether S-1 is bound to or dissociated from actin.

We previously referred to M·ADP·$P_{iI}$ and M·ADP·$P_{iII}$ as the refractory and the nonrefractory states, respectively (Stein et al., 1979, 1981). However, the term refractory state has become confused with our previous use of the term to mean refractory to binding to actin (Eisenberg & Kielley, 1972). Therefore, to avoid confusion, we will henceforth refer to the two postulated states as M·ADP·$P_{iI}$ and M·ADP·$P_{iII}$, respectively.

Although it contained an extra step, Stein et al. (1979) preferred the six-state kinetic model over the four-state kinetic model because it provided a simple explanation for a key aspect of the acto·S-1 ATPase data—the fact that the ATPase activity reaches 90% of its maximum value at an actin concentration where less than 50% of the S-1 is bound to actin. In quantitative terms, $K_{ATPase}$, the apparent binding constant determined from the double-reciprocal plot of ATPase activity vs. actin concentration, is stronger than $K_{BINDING}$, the binding constant determined from direct measurement of S-1 binding to actin in the presence of ATP. The six-state model could simultaneously account for the difference between $K_{ATPase}$ and $K_{BINDING}$ and predict a linear fit for the experimental double-reciprocal plot of ATPase activity vs. actin concentration. On the other hand, the four-state kinetic model could only account for the difference between $K_{ATPase}$ and $K_{BINDING}$ by approximating the linear double-reciprocal plot of ATPase vs. actin with a nonlinear plot (Stein et al., 1979).

In the present study, we investigated the nature of the rate-limiting step in the ATPase cycle by using both steady-state and pre-steady-state kinetic analysis. Our results conclusively show that $P_i$ release from A·M·ADP·$P_i$ cannot be the rate-limiting step in the ATPase cycle. Our results also suggest that the ATP hydrolysis step is not the rate-limiting step in the ATPase cycle. We therefore conclude that the four-state kinetic model cannot account for our kinetic data. Rather, the six-state model is required, which means that the rate-limiting step in the ATPase cycle is a conformational change in M·ADP·$P_i$ that occurs at about the same rate whether S-1 is bound to or dissociated from actin.

## Materials and Methods

Myosin was purified from rabbit back and leg muscles according to the method of Keilley & Harrington (1960). S-1 and (A-1)S-1 were prepared by the method of Weeds & Taylor (1975) except that 1 mM dithiothreitol was included in all of the solutions. F-Actin was prepared by a modified method of Spudich & Watt (1971) (Eisenberg & Keilley, 1974). Protein concentrations were measured spectrophotometrically. The extinction coefficents used for a 1 mg/mL solution at 280 nm were 0.75 $cm^{-1}$ for S-1 and (A-1)S-1 and 1.15 $cm^{-1}$ for F-actin (Eisenberg et al., 1968).

Measurements of the rate of fluorescence enhancement and turbidity change of acto·S-1 solutions were carried out in a stopped-flow apparatus as previously described (Stein et al., 1979). Quench-flow experiments were carried out in a Durram D-132 multimixer as previously described (Stein et al., 1979). ATPase activity was measured by either the pH stat technique or the direct assay of [$^{32}$P]$P_i$ production as described previously (Stein et al., 1981).

## Results

We first attempted to fit our steady-state and pre-steady-state kinetic data with the four-state kinetic model because it is simpler than the six-state kinetic model. As we discussed in the introduction, the key aspect of the steady-state ATPase data that must be fitted is the difference between $K_{ATPase}$ and $K_{BINDING}$. Stein et al. (1979) previously showed, with unfractionated S-1, that, at 15 °C, at very low ionic strength, $K_{ATPase}$ is about 4-fold stronger than $K_{BINDING}$. However, S-1, in fact, consists of a mixture of two isoenzymes, (A-1)S-1 and (A-2)S-1 (Weeds & Taylor, 1975). Each isoenzyme contains a different alkali light chain, and at low ionic strength, the two isoenzymes have different kinetic properties. In particular, $K_{ATPase}$ for (A-1)S-1 was found to be considerably stronger than that for (A-2)S-1 (Weeds & Taylor, 1975). To take advantage of the strong value for $K_{ATPase}$ obtained with (A-1)S-1 and to avoid possible artifacts stemming from the use of a mixture of isoenzymes, we employed (A-1)S-1 rather than unfractionated S-1 in the present study.

The solid circles in Figure 1 show a double-reciprocal plot of (A-1)S-1 ATPase activity vs. actin concentration. Unexpectedly, the double-reciprocal plot is not linear but shows about 30% inhibition at high actin concentration. This level of inhibition was consistently observed with a number of different preparations. However, the inset in Figure 1 shows that the inhibition does not exceed 30%, even when the actin concentration is increased from 100 to 320 $\mu$M. Therefore, although inhibition clearly occurs, the ATPase activity does

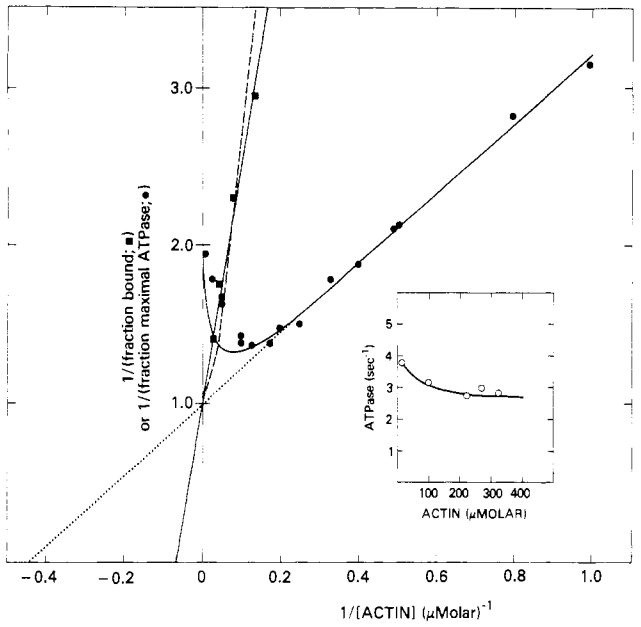


FIGURE 1: Steady-state binding of (A-1)S-1 to actin and steady-state ATPase activity. The steady-state ATPase activity has been normalized to the extrapolated $V_{max}$ (5 $s^{-1}$). Conditions were as follows: 10 mM imidazole, pH 7.0, 1.8 mM $MgCl_2$, 1 mM ATP, and 1 mM dithiothreitol, 15 °C. (●) Steady-state ATPase activity determined by pH stat titration; (■) fraction of (A-1)S-1 bound to actin during steady-state hydrolysis of ATP determined by stopped-flow turbidity. (Inset) (○) Steady-state ATPase activity at high actin concentration from direct determination of $[^{32}P]P_i$ production. (Dashed line) Predicted binding curve with four-state model (Scheme I) with $k_5$ = 21 $s^{-1}$, $k_{-5}$ = 7 $s^{-1}$, $k_6$ = 3 $s^{-1}$, $k_{-6}$ = 3 $s^{-1}$, $k_{10}$ = 80 $s^{-1}$, $K_3$ = 8.33 × $10^4$ $M^{-1}$, and $K_{13}$ = 2.78 × $10^4$ $M^{-1}$. See Figure 4 for predicted ATPase curves with four-state model. (Solid lines) Predicted curves with six-state model (Scheme II) with $k_5$ = 21 $s^{-1}$, $k_{-5}$ = 7 $s^{-1}$, $k_6$ = 27 $s^{-1}$, $k_{-6}$ = 27 $s^{-1}$, $k_7$ = 11 $s^{-1}$, $k_{-7}$ = 66 $s^{-1}$, $k_8$ = 6 $s^{-1}$, $k_{-8}$ = 36 $s^{-1}$, $k_{10}$ = 550 $s^{-1}$, $K_3$ = 1.11 × $10^5$ $M^{-1}$, and $K_{13}$ = $K_{14}$ = 3.7 × $10^4$ $M^{-1}$.

not decrease toward zero activity as the actin concentration is increased, as would be expected if it was necessary for S-1 to dissociate from actin during each cycle of ATPase hydrolysis.

Slight inhibition of the acto-S-1 ATPase activity at high actin concentration was previously observed by Marston (1978) for unfractionated S-1 at 0 °C. However, at 25 °C, Marston did not observe such inhibition, nor did we observe such inhibition with unfractionated S-1 at 15 °C. This may be because the amount of inhibition observed with (A-1)S-1 decreases somewhat as the temperature is increased and, in addition, over the range of actin concentration where inhibition of the (A-1)S-1 ATPase activity occurs, the (A-2)S-1 ATPase activity continues to increase (J. M. Chalovich et al., unpublished results).

We next studied the binding of (A-1)S-1 to actin in the presence of ATP. As in our previous work, binding was measured by the method of stopped-flow turbidity. The solid squares in Figure 1 show a double-reciprocal plot of the fraction of (A-1)S-1 bound to actin vs. actin concentration, and this plot yielded a value for $K_{BINDING}$ of 6.25 × $10^4$ $M^{-1}$, a value more than 6-fold weaker than the value of 4 × $10^5$ $M^{-1}$ obtained for $K_{ATPase}$. Therefore, for (A-1)S-1, as for unfractionated S-1, $K_{BINDING}$ is significantly weaker than $K_{ATPase}$, a phenomenon for which a complete kinetic model of the acto-S-1 ATPase activity must provide an explanation. Note that, although it is useful to characterize the difference between the binding and ATPase plots as a difference between $K_{ATPase}$ and $K_{BINDING}$, in matching our results to kinetic models, we

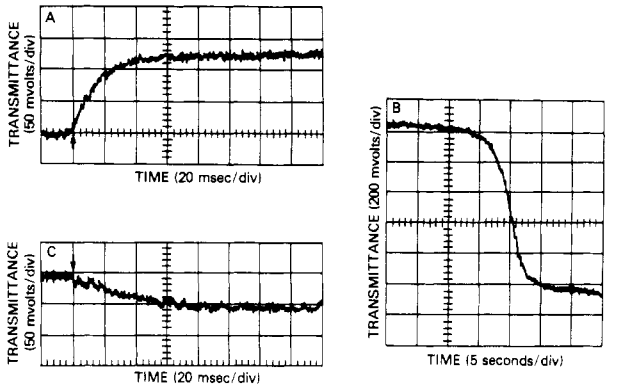


FIGURE 2: Pre-steady-state binding of (A-1)S-1 to actin. Conditions are the same as those in Figure 1. (A and B) (A-1)S-1 (20 μM) in one syringe was mixed with 42 μM actin + 2 mM ATP in the second syringe. Panel A shows the increase in light transmittance that occurs immediately after the flow stops (arrow). The increase in light transmittance represents a decrease in turbidity. Panel B shows the total decrease in light transmittance that occurs after the ATP is fully hydrolyzed. (C) (A-1)S-1 (20 μM) was briefly preincubated (1 min) with 2 mM ATP and then mixed with 44 μM actin. The arrow shows where the flow stopped. The decrease in light transmittance represents an increase in turbidity.

fitted the actual data (including the ATPase data at high actin concentration), not the extrapolated values for $K_{ATPase}$ and $K_{BINDING}$.

Before attempting to fit the ATPase and binding data with the four-state model, it was necessary to obtain more information about the rate constants and binding constants in the model. First, the individual binding constants of M·ATP and M·ADP·$P_i$ to actin had to be determined. Since S-1 occurs as a mixture of M·ATP and M·ADP·$P_i$ in the presence of ATP, $K_{BINDING}$ is a composite of the binding constants of M·ATP and M·ADP·$P_i$ to actin. Marston & Taylor (1980) suggested that M·ATP may bind significantly more tightly to actin than M·ADP·$P_i$, a conclusion that makes it easier to fit the kinetic data to the four-state model. In contrast, we previously suggested that the binding constants of M·ATP and M·ADP·$P_i$ to actin are nearly equal because stopped-flow turbidity experiments showed almost no change in binding occurred after S-1, ATP, and actin were mixed. However, we might have missed a small change in turbidity because unfractionated S-1 was used, which, in turn, required the experiments to be carried out at high actin concentrations where mixing tends to be slow. Therefore, we repeated these experiments with (A-1)S-1.

We previously showed that M·ATP and M·ADP·$P_i$ are in very rapid equilibrium with their respective actin complexes, A·M·ATP and A·M·ADP·$P_i$. Therefore, when S-1, actin, and ATP are mixed in a stopped-flow apparatus, an equilibrium mixture of M·ATP and A·M·ATP will form almost instantaneously, and any change in turbidity that occurs after mixing will be due to the formation of an equilibrium mixture of M·ADP·$P_i$ and A·M·ADP·$P_i$. Of course, a turbidity change will only occur if the equilibrium constant between M·ADP·$P_i$ and A·M·ADP·$P_i$ differs from the equilibrium constant between M·ATP and A·M·ATP; if the former binding constant is weaker than the latter, a decrease in turbidity will occur after mixing.

Figure 2A shows the results of an experiment where 10 μM (A-1)S-1 is reacted with 21 μM actin. Since $K_{BINDING}$ = 6.24 × $10^4$ $M^{-1}$ under these conditions, once steady state has been achieved, 50% of the (A-1)S-1 will be bound to actin, and the free actin concentration will be about 16 μM. As can be seen immediately after the mixing, there is indeed an increase in transmittance (decrease in turbidity) in this experiment. In

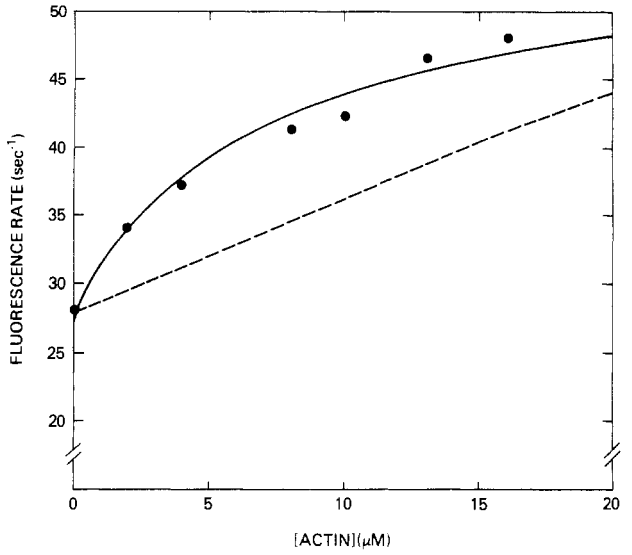


FIGURE 3: Rate of fluorescence enhancement as a function of actin concentration. Conditions are as in Figure 1. (●) Experimental data; (dashed line) prediction of four-state model with rate constants as in Figure 1; (solid line) prediction of six-state model with rate constants as in Figure 1.

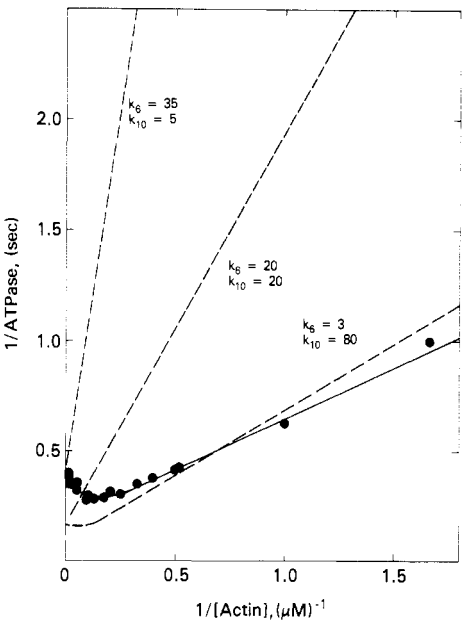


FIGURE 4: Theoretical plots predicted by the four-state model for ATPase activity. Conditions are as in Figure 1. The dashed lines represent theoretical plots prediced by the four-state model with varying ratios of $k_6$ to $k_{10}$ (see text). The solid line is the prediction of the six-state model with rate constants as in Figure 1. (●) Experimental data.

comparison, Figure 2B shows the transmittance change that occurs in this same experiment after all of the ATP is hydrolyzed. Since half of the (A-1)S-1 is bound to actin during steady-state ATP hydrolysis, this final transmittance change (1200 mV) represents about half of the total transmittance change that would be caused by the binding of all of the (A-1)S-1 to actin (2400 mV). The decrease in transmittance in Figure 2A (120 mV) is about 5% of this total transmittance change; therefore, about 5% of the (A-1)S-1 dissociates from actin as the M·ATP transforms to M·ADP·$P_i$. Even if, because of mixing delays, this represents only half of the real change and even if only half of the (A-1)S-1 occurs as M·ADP·$P_i$ during this experiment, this result means that, at most, M·ATP binds 3-fold stronger to actin than M·ADP·$P_i$.

If this is indeed the case, a decrease in transmittance (increase in turbidity) should occur when M·ADP·$P_i$ is mixed with actin since the equilibrium mixture of M·ADP·$P_i$ and A·M·ADP·$P_i$ will shift back toward M·ATP and A·M·ATP. This experiment is carried out by premixing S-1 with ATP prior to introducing it into the stopped-flow apparatus; the S-1 in this mixture is about 75% M·ADP·$P_i$ and 25% M·ATP. As can be seen in Figure 2C, when this solution is mixed with actin, there is indeed a small but reproducible decrease in transmittance. This effect is too small to be analyzed quantitatively, but it qualitatively confirms that M·ATP could bind more strongly to actin than M·ADP·$P_i$. Therefore, in fitting our data to the four-state model, we make the most favorable assumption for this model; we assume that $K_3$ is 3-fold stronger than $K_{13}$.

Before fitting our data to the four-state kinetic model, it was also necessary to determine the rate of the ATP hydrolysis step as a function of actin concentration. This rate was determined by measuring the rate of the fluorescence increase that occurs when S-1 is mixed with 2 mM ATP at varying actin concentration. This fluorescence increase has previously been shown to be due to the transition from M·ATP to M·ADP·$P_i$ (Johnson & Taylor, 1978; Chock et al., 1979). Our previous data with unfractionated S-1 (Stein et al., 1981) or with fluorescently labeled S-1 (Marsh et al., 1982) suggested that the rate of the ATP hydrolysis step increased with increasing actin concentration, and Figure 3 shows that the same effect occurs with (A-1)S-1.

In the absence of actin, the rate constant for the fluorescence increase is about 28 $s^{-1}$ for (A-1)S-1. Since quench-flow experiments show that the equilibrium constant between M·ATP and M·ADP·$P_i$ is about 3, the forward rate of the ATP hydrolysis step ($k_5$ in Scheme I) is about 21 $s^{-1}$, and the reverse rate ($k_{-5}$ in Scheme I) is about 7 $s^{-1}$. In the presence of actin, the fluorescence rate approaches 50 $s^{-1}$ at 20 $\mu$M actin. However, this rate constant is not just affected by the sum of the forward and reverse rate constants of the ATP hydrolysis step that occurs with S-1 bound to actin ($k_6 + k_{-6}$ in Scheme I). It also includes the rate of $P_i$ release from A·M·ADP·$P_i$ ($k_{10}$ in Scheme I) since, during steady-state ATP hydrolysis, this step provides an alternate pathway from A·M·ADP·$P_i$ back to A·M·ATP. Therefore, these fluorescence data require that the quantity $k_6 + k_{-6} + k_{10}$ in Scheme I have a value (about 80 $s^{-1}$) that allows the observed fluorescence rate to be about 50 $s^{-1}$ at 20 $\mu$M actin.

We now had enough information to computer fit our data using the four-state kinetic model. The binding constants $K_3$ and $K_{13}$ were set so that, on average, $K_{BINDING} = 6 \times 10^4$ $M^{-1}$ and $K_3 = 3K_{13}$. In addition, $k_5$ was set equal to 21 $s^{-1}$, $k_{-5}$ was set equal to 7 $s^{-1}$, and $k_6 + k_{-6} + k_{10}$ was set equal to approximately 80 $s^{-1}$. The only remaining variable in the model was the ratio of $k_6$ to $k_{10}$, where $k_6$ is the rate constant for the ATP hydrolysis step and $k_{10}$ is the rate constant for $P_i$ release when S-1 is completely bound to actin.

The dashed lines in Figure 4 show the fit of the four-state model to the ATPase data at varying ratios of $k_6$ to $k_{10}$. As can be seen, the model can only fit the data if the rate constant for $P_i$ release ($k_{10}$) is much faster than the rate constant for $P_i$ hydrolysis ($k_6$). When $P_i$ release is made rate limiting, the extrapolated value for $K_{ATPase}$ is approximately equal to $K_{BINDING}$ ($6 \times 10^4$ $M^{-1}$). Only if the ATP hydrolysis step is rate limiting can the model fit the ATPase data reasonably well. The best fit was obtained by setting $K_3 = 8.3 \times 10^4$ $M^{-1}$, $K_{13} = 2.8 \times 10^4$ $M^{-1}$, $k_6 = 3$ $s^{-1}$, and $k_{10} = 80$ $s^{-1}$. The fit to the binding and fluorescence data with these parameters is given by the dashed lines in Figures 1 and 3; the fit is reasonable although not perfect. Extensive modeling with other

Table I: Determination of the Magnitude of the $P_i$ Burst[a]

| actin concn (M) | steady-state rate ($s^{-1}$)[b] | total counts at 128 ms | counts due to steady-state rate at 128 ms[c] | magnitude of $P_i$ burst[d] |
|---|---|---|---|---|
| 0 | | 3326 | | 0.7 |
| 21 | 3.6 | 5237 | 2678 | 0.54 |
| 39 | 4.1 | 5094 | 3136 | 0.41 |
| 72 | 3.5 | 4337 | 2668 | 0.35 |
| 50[e] | 0.7 | 3540 | 499 | 0.64 |

[a] Conditions are as in Figure 1, except that here the ATP concentration is 0.1 mM, and 1.8 mM KCl has been added to keep the ionic strength the same as that in Figure 1. [b] The steady-state rate was determined by using the aging mode of the quench-flow apparatus and comparing the phosphate released at 160 and 1160 ms. In the aging mode, the S-1 actin and ATP were mixed, and then a 1-s delay was imposed before the solution was quenched by acid from the third syringe. [c] By use of the steady-state rate determined in footnote *b*, the counts due to this rate at 128 ms were calculated. [d] The magnitude of the burst was determined by subtracting the counts given in footnote *c* from the total counts given in footnote *b* and then dividing the result by the specific activity of the ATP and by the concentration of S-1 present. [e] In this experiment, regulated actin (including 10 μM troponin–tropomyosin) was used, and 1 mM EGTA was present.

ratios of $K_3$ to $K_{13}$ from 1 to 10 gave similar results. Only if the rate constant for $P_i$ release is set markedly greater than the rate constant for the ATP hydrolysis step can this model account for the experimental difference between $K_{ATPase}$ and $K_{BINDING}$. We therefore conclude that, if the four-state model is valid, $P_i$ release from A·M·ADP·$P_i$ cannot be the rate-limiting step in the actomyosin ATPase cycle; for this model to be valid, the ATP hydrolysis step with S-1 bound to actin ($k_6$) must be rate limiting under our experimental conditions.

The assumption that the transition from A·M·ATP to A·M·ADP·$P_i$ ($k_6$) is the rate-limiting step in the actomyosin ATPase cycle leads to a simple prediction: very little A·M·ADP·$P_i$ should form after ATP is mixed with S-1 at high actin concentration and, similarly, very little A·M·ADP·$P_i$ should be present during steady-state ATP hydrolysis at high actin concentration. This is because, if $P_i$ release is much faster than the ATP hydrolysis step, $P_i$ will dissociate from A·M·ADP·$P_i$ much faster than A·M·ADP·$P_i$ is formed. Unfortunately, it is difficult to accurately measure the amount of A·M·ADP·$P_i$ formed (the initial $P_i$ burst) when S-1 is mixed with ATP at high actin concentration. Mixing is difficult because the high actin concentration makes the solution viscous. In addition, the steady-state ATPase rate itself is quite rapid, and measurement of the amount of A·M·ADP·$P_i$ formed requires determination of the amount of $P_i$ formed over and above the amount formed during steady-state ATP hydrolysis.

In experiments to determine the amount of A·M·ADP·$P_i$ present at high actin concentration, both the steady-state and pre-steady-state $P_i$ production were measured in the quench-flow apparatus. The steady-state $P_i$ production was measured at two or three time points between 160 and 1160 ms while the pre-steady-state $P_i$ production (initial $P_i$ burst) was measured at 120 and 160 ms. Table I shows that at both low and high actin concentration "extra" $P_i$ is produced at the early time points. Although the effect is not large, it has consistently been observed in our experiments. Table I also shows a control experiment performed in the presence of EGTA [ethylene glycol bis(β-aminoethyl ether)-*N*,*N*,*N*′,*N*′-tetraacetic acid] and troponin–tropomyosin. Here, the actin-activated ATPase rate is partially "turned off" by the troponin–tropomyosin (although not completely because of the high S-1 concentration present),

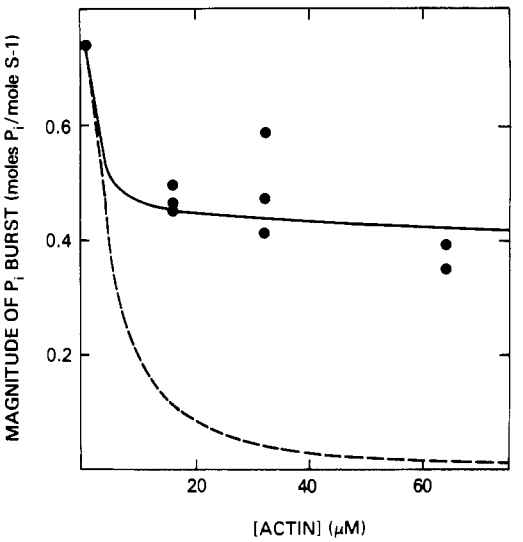


FIGURE 5: Magnitude of the phosphate burst as a function of actin concentration. Conditions are as in Figure 1, except final ATP concentration equaled 0.10 mM and 1.8 mM KCl has been added to keep the ionic strength the same as that in Figure 1. (●) Experimental data obtained with several different preparations of (A-1)S-I; (dashed line) prediction of four-state model with rate constants as in Figure 1; (solid line) prediction of the six-state model with rate constants as in Figure 1.

and therefore, the magnitude of the extra $P_i$ produced can be determined more accurately than in the experiments without troponin–tropomyosin. As can be seen, a quite reasonable value for the magnitude of the initial $P_i$ burst is obtained in this control experiment with troponin–tropomyosin present, which suggests that our technique for measuring the initial $P_i$ burst in the presence of actin is valid.

The solid circles in Figure 5 summarize the data obtained in similar experiments carried out at a number of different actin concentrations in the absence of troponin–tropomyosin. As can be seen, there is some variability in the data, and there does appear to be a decrease in the magnitude of the initial $P_i$ burst at high actin concentration. Nevertheless, the measured magnitude of the $P_i$ burst is much greater than the value predicted by the four-state model (dashed line in Figure 5).

Because of the difficulty in directly measuring the magnitude of the initial $P_i$ burst, we also used the tryptophan fluorescence to measure the ratio of A·M·ADP·$P_i$ to A·M·ATP. When S-1 is mixed with relatively high concentrations of ATP, essentially all of the fluorescence increase that is observed is due to the transition from M·ATP to M·ADP·$P_i$ (Johnson & Taylor, 1978; Chock et al., 1979). Therefore, in theory, by determination of this increase in fluorescence in the presence and absence of actin, the amount of A·M·ADP·$P_i$ present during steady-state ATP hydrolysis can be estimated, under the assumption, of course, that the transition from A·M·ATP to A·M·ADP·$P_i$ gives the same fluorescence increase as the transition from M·ATP to M·ADP·$P_i$. On this basis, under conditions where S-1 is half-bound to actin, the four-state model predicts that the fluorescence increase will be 35% of that with S-1 alone while the six-state model predicts that it will be 66% of that with S-1 alone (see Appendix). Unfortunately, in the presence of actin, the sample solution has a high viscosity, and in addition, the rate of the fluorescence increase is quite high. Therefore, it is difficult to accurately estimate the magnitude of the fluorescence increase. Generally, under conditions where half of the S-1 is bound to actin, we observed a fluorescence increase about 50% of that obtained with S-1 alone, but it is likely that the early part of the

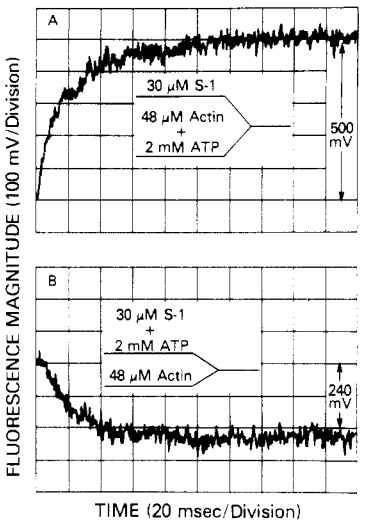


FIGURE 6: Magnitude of the fluorescence enhancement. Conditions are as in Figure 1. Panel A shows the rise in fluorescence that occurred following the addition of 30 μM (A-1)S-1 to 48 μM actin + 2 mM ATP. Panel B shows the fall in fluorescence that occurred when 30 μM (A-1)S-1 was briefly incubated with 2 mM ATP (1 min) and then mixed with 48 μM actin.

fluorescence trace was not observed due to the inherent dead time of the instrument.

One way around this problem is to compare the rise in fluorescence that occurs when S-1, actin, and ATP are mixed together with the fall in fluorescence that occurs when M·ADP·$P_i$ is mixed with actin. Here, any loss of signal should be the same in both experiments. These experiments are identical with the experiments shown in Figure 2 except that here fluorescence is measured rather than turbidity. When S-1 is mixed with actin and ATP, 100% of the S-1 occurs as M·ATP and A·M·ATP at time zero. On the other hand, when S-1 and ATP are premixed to form M·ATP and M·ADP·$P_i$ and then mixed with actin, 75% of the S-1 occurs as M·ADP·$P_i$ and A·M·ADP·$P_i$ and 25% as M·ATP and A·M·ATP at time zero. Under conditions where half of the (A-1)S-1 is bound to actin, the four-state model predicts that 25% of the S-1 will occur as M·ADP·$P_i$ and A·M·ADP·$P_i$ during steady-state ATP hydrolysis, while the six-state model predicts that 50% of the S-1 will occur as M·ADP·$P_i$ and A·M·ADP·$P_i$ (see Appendix). Therefore, in this experiment, the four-state model predicts that the rise in fluorescence (caused by the ADP·$P_i$ species going from 0 to 25% of the total S-1) will be *half* the fall in fluorescence (caused by the ADP·$P_i$ species going from 75 to 25% of the total S-1). On the other hand, the six-state model predicts that the rise in fluorescence (caused by the ADP·$P_i$ species going from 0 to 50% of the total S-1) will be *twice* the fall in fluorescence (caused by the ADP·$P_i$ species going from 75 to 50% of the total S-1).

The results of this experiment are shown in Figure 6. As can be seen, the rise in fluorescence is indeed about twice the fall in fluorescence, which is consistent with the six-state model. Note that the results of this experiment do not depend on the specific fluorescence of A·M·ATP or A·M·ADP·$P_i$. Since M·ATP and A·M·ATP are in rapid equilibrium, they essentially act as one species, and the same is true for M·ADP·$P_i$ and A·M·ADP·$P_i$. As long as the fluorescence magnitude of M·ADP·$P_i$ + A·M·ADP·$P_i$ is greater than the fluorescence magnitude of M·ATP + A·M·ATP, the result will be the same (see Appendix). We conclude that, like the direct measurement of the $P_i$ burst, this measurement of the fluorescence change suggests that the amount of M·ADP·$P_i$ and A·M·ADP·$P_i$ present during steady-state ATP hydrolysis is considerably greater than would be predicted by the four-state model.

## Discussion

Two conclusions can be drawn from the results presented in this paper. First, it is clear that, at very low ionic strength, at 15 °C, $K_{ATPase}$ is significantly stronger than $K_{BINDING}$ for (A-1)S-1; that is, half-maximal ATPase activity occurs at a significantly lower actin concentration than half-maximal binding of (A-1)S-1 to actin. This phenomenon has previously been observed (Wagner & Weeds, 1979). When it was first observed by Eisenberg & Kielley (1972), it was misinterpreted to mean that almost no S-1 was bound to actin when the ATPase activity was at $V_{max}$. Obviously, this interpretation of the data was incorrect. Nevertheless, the experimental difference between $K_{ATPase}$ and $K_{BINDING}$ is real, and recently, a similar difference has been observed with smooth muscle S-1 at 25 °C at low ionic strength (Greene et al., 1983). On the other hand, a similar difference between $K_{ATPase}$ and $K_{BINDING}$ was not observed with smooth muscle HMM (Sellers et al., 1982), and furthermore, even with skeletal muscle S-1 this difference appears to decrease as the temperature is increased (Wagner & Weeds, 1979). Therefore, a kinetic model for the acto·S-1 ATPase activity must be able to account both for the large difference between $K_{ATPase}$ and $K_{BINDING}$ at low temperature and for a decrease in this difference as the temperature is increased.

The second conclusion we can draw from the data presented in this paper is that, under conditions where $K_{ATPase} > K_{BINDING}$, $P_i$ release from A·M·ADP·$P_i$ is not the rate-limiting step in the ATPase cycle. If $P_i$ release were the rate-limiting step in the ATPase cycle, $K_{ATPase}$ would have to be nearly equal to $K_{BINDING}$. Therefore, some other step in the cycle must be rate limiting.

The only other step in the four-state model that can be rate limiting is the ATP hydrolysis step, A·M·ATP → A·M·ADP·$P_i$. In this case, the subsequent release of $P_i$ must occur quite rapidly both to account for the increase in the fluorescence enhancement rate caused by actin (Figure 3) and to account for $K_{ATPase}$ being greater than $K_{BINDING}$. In effect, increasing the rate constant for $P_i$ release ($k_{10}$) "pulls" the ATPase cycle around by increasing the rate constant for the overall transition from M·ADP·$P_i$ to A·M·ADP + $P_i$ ($k_{10}k_{13}$[A]). As the value for this rate constant increases, the actin concentration required for half-maximal ATPase activity decreases, and therefore, $K_{ATPase}$ increases compared to $K_{BINDING}$.

If the step A·M·ATP → A·M·ADP·$P_i$ is rate limiting and $P_i$ release is quite rapid, very little A·M·ADP·$P_i$ will form and be present during steady-state ATP hydrolysis at high actin concentration. As fast as A·M·ADP·$P_i$ is formed, it will be depleted by the rapid $P_i$ release. Therefore, this model can be tested by measuring the amount of A·M·ADP·$P_i$ formed after actin, ATP, and S-1 are mixed in a quench-flow apparatus, i.e., by measuring the magnitude of the initial $P_i$ burst in the presence of high actin concentration. The results in this paper, obtained both by direct measurement and by measurement of relative fluorescence magnitude, suggest that too much A·M·ADP·$P_i$ occurs for the *formation* of A·M·ADP·$P_i$ to be the rate-limiting step in the ATPase cycle. Clearly, these experiments are difficult and cannot be considered absolutely definitive. However, preliminary experiments with cross-linked S-1 (Stein et al., 1983) tend to substantiate these conclusions, and therefore, we consider it unlikely that the four-state model can account for our data. We think it more likely that the six-state model is the simplest model that can account for the acto·S-1 ATPase data.

The key point in the six-state model is that the ATP hydrolysis step is followed, not by $P_i$ release, but rather by a rate-limiting conformational change, which, like the ATP hydrolysis step, occurs both when the S-1 is bound to and dissociated from actin. The rapid release of $P_i$ from A·M·ADP·$P_i$ then occurs after the rate-limiting step. Since the rapid release of $P_i$ is separated from the ATP hydrolysis step by the intervening rate-limiting step, this model predicts a larger amount of A·M·ADP·$P_i$ will be present during steady-state ATP hydrolysis than is predicted by the four-state model. At the same time, the model accounts for the difference between $K_{ATPase}$ and $K_{BINDING}$ because rapid $P_i$ release directly follows a rate-limiting step, which occurs both when the S-1 is bound to and dissociated from actin. Thus, the rapid $P_i$ release pulls the ATPase cycle around making $K_{ATPase} > K_{BINDING}$.

By use of the following values for rate constants and binding constants, the six-state kinetic model can account for the data presented in this paper as shown by the solid lines in Figures 1 and 3–5: $k_5 = 21\ s^{-1}$, $k_{-5} = 7\ s^{-1}$, $k_6 = 27\ s^{-1}$, $k_{-6} = 27\ s^{-1}$, $k_7 = 11\ s^{-1}$, $k_{-7} = 66\ s^{-1}$, $k_8 = 6\ s^{-1}$, $k_{-8} = 36\ s^{-1}$, $k_{10} = 550\ s^{-1}$, $K_3 = 1.1 \times 10^5\ M^{-1}$, $K_{13} = 3.7 \times 10^4\ M^{-1}$, and $K_{14} = 3.7 \times 10^4\ M^{-1}$. Note that we have made $k_7$ about 2-fold greater than $k_8$; this was done to match the decrease in ATPase rate that occurs at high actin concentration with (A-1)S-1 at 15 °C. With (A-2)S-1 where this inhibition does not occur, $k_7$ may equal $k_8$. Note also that this set of kinetic values may not be unique; other sets of values might also be able to account for our experimental data. Furthermore, temperature may affect the values of several of these rate constants, which could explain the effect of temperature on the ratio of $K_{ATPase}$ to $K_{BINDING}$.

One property of the actomyosin ATPase cycle that neither the four-state model nor the six-state model can readily account for is the absence of intermediate $^{18}O$ exchange at high actin concentration (Sleep & Boyer, 1978). $^{18}O$ exchange is thought to be caused by a combination of rotation of $P_i$ at the active site and repeated reversals of the ATP hydrolysis step before $P_i$ is released from the active site. On this basis, at high actin concentration, the amount of $^{18}O$ exchange should depend on the ratio of $k_{-6}$ to $k_{10}$ in the four-state model and on the ratio of $k_{-6}$ to $k_8$ in the six-state model. Since at 15 °C $k_{10}$ in the four-state model is assumed to be much faster than $k_8$ in the six-state model, it would at first appear that the four-state model could account for the absence of $^{18}O$ exchange at high actin concentration more simply than the six-state model. However, under conditions where $k_{10}$ is much greater than $k_{-6}$, the four-state model not only explains the absence of $^{18}O$ exchange but also predicts that $K_{ATPase}$ will be much greater than $K_{BINDING}$. Since at 25 °C the difference between $K_{ATPase}$ and $K_{BINDING}$ decreases markedly, the difference between $k_{10}$ and $k_{-6}$ must also decrease. Therefore, at 25 °C, neither the four-state nor the six-state model can simply account for the absence of $^{18}O$ exchange at high actin concentration. An alternative explanation for this phenomenon is that bound actin interferes with the rotation of $P_i$ at the active site. We are presently investigating this possibility.

It is of interest to consider the physiological significance of this model. In simplest terms, the model suggests that myosin exists in two major conformational states: a weak-binding state that occurs with ATP or ADP + $P_i$ bound at the active site and a strong-binding state that occurs either in the absence of nucleotide or with ADP bound at the active site. The model also suggests that the rate-limiting step occurs before the transition from the weak-binding to the strong-binding state. Therefore, in solution, almost all of the S-1 occurs in the weak-binding state during steady-state ATP hydrolysis.

It is possible that, in muscle, the myosin cross-bridge also oscillates back and forth between the weak and strong binding states (Eisenberg & Greene, 1980). However, in muscle, the rate-limiting step cannot simply be a conformational change that occurs prior to formation of the strong binding state. Both in the isometric and isotonic states (except at maximum velocity) the muscle exerts force, and myosin cross-bridges in the weak binding state could not exert significant force; they would detach from actin if they were significantly stressed. Therefore, in muscle, a significant number of myosin cross-bridges (but not all) apparently exist in a strong binding state where they exert positive force. This, in turn, suggests that in muscle there may be two slow steps in the ATPase cycle: a step that controls the rate at which the cross-bridge enters the major force-producing state and a step that controls the rate at which the cross-bridge leaves the major force-producing state. These two steps would be analogous to $f$ and $g$ in the 1957 model of Huxley (1957). *Both* steps would control the shape of the force–velocity curve, and a balance between the two steps would ensure that some, but not all, of the cross-bridges were in the major force-producing state during muscle shortening.

In the 1957 model of A. F. Huxley, $f$ was the rate of attachment of the cross-bridge to actin. However, our kinetic model suggests that S-1 attaches to and detaches from actin very rapidly when it is in the weak binding state, and recent data suggest that a similar phenomenon occurs in muscle fibers (Brenner et al., 1982). Therefore, it seems more likely that $f$ is analogous to the rate-limiting step in the ATPase cycle, which controls the rate of the transition from the weak binding state to the strong binding state. Although we have determined the value of this rate-limiting step at low ionic strength, experiments with S-1 cross-linked to actin (Mornet et al., 1981) suggest that this rate-limiting step is not significantly affected by ionic strength (L. A. Stein et al., unpublished data). In addition, computer modeling suggests that the value of this rate-limiting step is of the right order of magnitude to account for the shape of the force–velocity curve (Eisenberg et al., 1980). If this is indeed the case, it could explain the correlation that has been observed (Barany, 1967) between the shortening velocity of various types of muscles and the actin-activated ATPase rates. In addition, it predicts that the rate at which a cross-bridge redevelops force after detaching from actin in the muscle fiber should be equal to the maximum actin-activated ATPase rate determined from the double-reciprocal plot of ATPase activity vs. actin concentration. We are currently testing this prediction.

In conclusion, we have shown that $P_i$ release is not the rate-limiting step in the acto·S-1 ATPase cycle and have also presented evidence suggesting that the hydrolysis step itself is not rate limiting. Instead, a conformational change that follows hydrolysis but precedes $P_i$ release appears to be rate limiting; like the hydrolysis step, it seems to occur at about the same rate whether the S-1 is bound to or dissociated from actin. This rate-limiting step may control the rate at which the myosin cross-bridge enters the major force-producing state in vivo and thus may be a key determinant of the force–velocity curve for various types of muscle.

## Appendix

*Theoretical Determination of $P_i$ Burst Magnitude. (A) Four-State Model (Scheme I).* If one assumes that $K_3$ and $K_{13}$ represent rapid equilibria, the four-state model reduces to a two-state model ([ATP] assumed to be saturating). Note that in these equations $K_3$ and $K_{13}$ are dissociation constants.

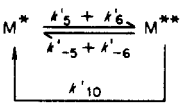


(1)

$M^* = [M{\cdot}T] + [AM{\cdot}T]$, $M^{**} = [M{\cdot}D{\cdot}P_i] + [AM{\cdot}D{\cdot}P_i]$ (T = ATP, D = ADP), $k'_5 = k_5K_3/(K_3 + [A])$, $k'_6 = k_6[A]/(K_3 + [A])$, $k'_{-6} = k_{-6}[A]/(K_{13} + [A])$, $k'_{-5} = k_{-5}K_{13}/(K_{13} + [A])$, and $k'_{10} = k_{10}[A]/(K_{13} + [A])$. The differential equation and mass conservation equations are given by

$$dM^{**}/dt = M^*(k'_5 + k'_6) - M^{**}(k'_{-5} + k'_{-6} + k'_{10})$$

$$M_T = M^* + M^{**}$$

where $M_T$ = total myosin. The solution is

$$M^{**} = \frac{M_T(k'_5 + k'_6)}{(k'_5 + k'_6 + k'_{-5} + k'_{-6} + k'_{10})}(1 - e^{-(k'_5+k'_{-5}+k'_6+k'_{-6}+k'_{10})t}) \quad (2)$$

To calculate the magnitude of the initial phosphate burst, it is necessary to calculate the phosphate measured as a function of time:

$$P_{meas}(t) = k'_{10}\int M^{**}(t)\,dt + M^{**}(t)$$

or

$$P_{meas}(t) = \frac{k'_{10}M_T(k'_5 + k'_6)t}{(k'_5 + k'_6 + k'_{-5} + k'_{-6} + k'_{10})} + \frac{M_T(k'_5 + k'_6)(k'_5 + k'_6 + k'_{-5} + k'_{-6})}{(k'_5 + k'_6 + k'_{-6} + k'_{-6} + k'_{10})^2}(1 - e^{-\Sigma t}) \quad (3)$$

where $\Sigma = k'_5 + k'_6 + k'_{-5} + k'_{-6} + k'_{10}$. The first term is $M_TV_{ss}t$, where $V_{ss}$ is the steady-state rate. The magnitude of the initial $P_i$ burst is then defined by

$$\text{magnitude of } P_i \text{ burst} = \text{limit}(t\to\infty)\ \frac{P_{meas}(t) - M_TV_{ss}t}{M_T} \quad (4)$$

Note that because of the correction for the steady-state rate, this magnitude is less than the amount of $M^{**}$ ($M{\cdot}D{\cdot}P_i$ + $AM{\cdot}D{\cdot}P_i$) present during steady-state ATP hydrolysis.

*(B) Six-State Model (Scheme II).* The six-state model is more complex, but can be solved similarly. We make the assumption that $K_{14}$ represents a rapid equilibrium and that $k_{10}$ is in this case given by $k_{10}[A]/(K_{14} + [A])$, and with the additional definitions $k'_7 = k_7K_{13}/(K_{13} + [A])$, $k'_8 = k_8[A]/(K_{13} + [A])$, $k'_{-7} = k_{-7}K_{14}/(K_{14} + [A])$, and $k'_{-8} = k_{-8}[A]/(K_{14} + [A])$, the six-state model reduces to

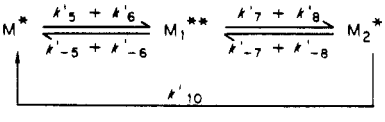


(5)

The solution to the differential equations is as follows:

$$M_1^{**}(t) = C_1e^{\lambda_+t} + D_1e^{\lambda_-t} + \frac{A_2Q_1}{A_2B_1 - A_1B_2} \quad (6)$$

$$M_2^{**}(t) = C_2e^{\lambda_+t} + D_2e^{\lambda_-t} + \frac{B_2Q_1}{B_1A_2 - A_1B_2}$$

$$M^*(t) = M_T - M_1^{**} - M_2^{**}$$

where $Q_1 = (k'_5 + k'_6)M_T$, $A_1 = k'_{-7} + k'_{-8} - k'_5 - k'_6$, $B_1 = k'_{-5} + k'_{-6} + k'_5 + k'_6 + k'_7 + k'_8$, $B_2 = k'_7 + k'_8$, $A_2 = k'_{-7} + k'_{-8} + k'_{10}$, $\lambda_\pm = (-(B_1 + A_2) \pm [(B_1 + A_2)^2 + 4(A_1B_2 - A_2B_1)]^{1/2})/2$, and

$$D_1 = \frac{Q_1}{\lambda_- - \lambda_+}\left(1 + \frac{\lambda_+A_2}{A_2B_1 - B_2A_1}\right)$$

$$D_2 = \frac{\lambda_+}{\lambda_- - \lambda_+}\frac{B_2Q_1}{A_2B_1 - B_2A_1}$$

$$C_1 = \frac{-Q_1}{\lambda_- - \lambda_+}\left(1 + \frac{A_2\lambda_-}{A_2B_1 - B_2A_1}\right)$$

$$C_2 = -\frac{\lambda_-}{\lambda_- - \lambda_+}\frac{B_2Q_1}{A_2B_1 - B_2A_1}$$

In this case, the phosphate measured is given by

$$P_{meas}(t) = k'_{10}\int M_2^{**}(t)\,dt + M_1^{**}(t) + M_2^{**}(t)$$

and the magnitude of the initial $P_i$ burst is defined as in the four-state model:

$$\text{magnitude of } P_i \text{ burst} \equiv \text{limit}(t\to\infty)\ \frac{P_{prod}(t) - V_{ss}M_Tt}{M_T}$$

and is given by

$$\text{magnitude of } P_i \text{ burst} = \frac{(A_2 + B_2)Q_1/M_T}{A_2B_1 - A_1B_2} - \frac{k'_{10}}{M_T}\left(\frac{C_2}{\lambda_+} + \frac{D_2}{\lambda_-}\right) \quad (7)$$

As is the case with the four-state model, this magnitude is less than the amount of $M_1^{**} + M_2^{**}$ present during steady-state ATP hydrolysis.

*Theoretical Determination of Fluorescence Magnitude.* In order to directly compare the fluorescence magnitudes predicted by the four- and six-state models with the fluorescence magnitude in the absence of actin an assumption concerning the relative fluorescence associated with the states $M{\cdot}D{\cdot}P_i$ and $AM{\cdot}D{\cdot}P_i$ is made, namely, that the fluorescence enhancements are equal. With this assumption, the fluorescence magnitude directly reflects the occupation of the state $M^{**}$ ($M{\cdot}D{\cdot}P_i$ + $AM{\cdot}D{\cdot}P_i$). The predicted magnitudes can therefore be determined from eq 2 (four-state model) or from $M_1^{**} + M_2^{**}$ in eq 6 (six-state model).

When (A-1)S-1 is reacted with ATP in the absence of actin at 15 °C and 0.013 M ionic strength, the steady-state fractional occupation of the state $M{\cdot}D{\cdot}P_i$ is 0.75. That is, 75% of the myosin species is in the state $M{\cdot}D{\cdot}P_i$ at steady state. Under the same conditions when (A-1)S-1 is reacted with ATP in the presence of 16 $\mu$M free actin, eq 2 predicts that about 27% of the myosin will be in the state $M^{**}$ at steady state. Therefore, the fluorescence signal at 16 $\mu$M actin is predicted to be 35% of the signal at zero actin. On the other hand, on the basis of the rate constants given under Discussion, the six-state model predicts that about 50% of the myosin will be in the state $M_1^{**}$ ($M_2^{**}$ assumed to be negligible) at 16 $\mu$M actin during the steady state, implying that the fluorescence signal observed should be about 67% of that observed in the absence of actin. As discussed under Results, the direct measurement of the fluorescence was found to be midway between these estimates.

A second method for estimating the occupation of the $M^{**}$ state is discussed in the text. In this method, the fluorescence enhancement measured when S-1 is mixed with actin + ATP is compared to the fall in fluorescence when actin is mixed with S-1 + ATP. The interpretation of these data does not require the assumption that $M{\cdot}D{\cdot}P_i$ and $AM{\cdot}D{\cdot}P_i$ show the same fluorescence enhancement relative to M·D and AM·T, respectively.

Refer now to Scheme I. We continue to assume the concentration of $M_2$** is negligible compared to $M_1$**, and therefore, in the situation discussed here, it suffices to examine only the four-state model. Consider first the mixing of S-1 + ATP with actin. Under these conditions at $t = 0$ (prior to mixing), 75% of the S-1 is in the state M·D·$P_i$ and 25% is in the state M·T. At $t = 0^+$, immediately after mixing, 75% of the S-1 will be in the state M** (M·D·$P_i$ + AM·D·$P_i$) and 25% of the S-1 will be in state M* (M·T + AM·T) due to the rapid equilibrium binding that occurs. Let $f_T = [A]/(K_3 + [A])$ and $f_D = [A]/(K_{13} + [A])$, then at $t = 0$ the fractional partitioning of the states will be as follows:

$$AM\cdot T/M_{total} = 0.25f_T \qquad AM\cdot D\cdot P_i/M_{total} = 0.75f_D$$

$$M\cdot T/M_{total} = 0.25(1 - f_T)$$

$$M\cdot D\cdot P_i/M_{total} = 0.75(1 - f_D)$$

where $M_{total}$ = total myosin. Let $x$, $y$, $nx$, and $\gamma y$ be the fluorescence enhancement associated with the states M·T, M·D·$P_i$, AM·T, and AM·D·$P_i$, respectively. Since $n$ and $\gamma$ are not specified, we are assuming nothing about the relative fluorescence magnitudes. The fluorescence signal at $t = 0$ immediately after mixing for the technique of mixing described above is given by

$$F_1(t = 0) = 0.25x(1 - f_T + nf_T) + 0.75y(1 - f_D + \gamma f_D)$$

At steady state, a certain fraction $\rho$ of the total myosin will be in the states AM·D·$P_i$ and M·D·$P_i$, and the steady-state fluorescence is given by

$$F_1(\text{steady state}) = x(1 - \rho)(1 - f_T + nf_T) + \rho y(1 - f_D + \gamma f_D)$$

The change in fluorescence observed between steady state and $t = 0$ is therefore

$$\Delta_1 \equiv F_1(\text{steady state}) - F_1(t = 0) = [x(1 - f_T + nf_T) - y(1 - f_D + nf_D)](0.75 - \rho)$$

Consider now the experiment in which S-1 is mixed with actin + ATP. Due to rapid equilibrium binding, at $t = 0$, 100% of the S-1 will be in the state M** (M·T + AM·T) with fractional partition

$$AM\cdot T/M_{total} = f_T \qquad M\cdot T/M_{total} = 1 - f_T$$

The initial fluorescence is therefore

$$F_2(t = 0) = x(1 - f_T + nf_T)$$

The fluorescence at steady state in this case is the same as in the first technique of mixing, $F_1$(steady state); therefore, the change in fluorescence observed is given by

$$\Delta_2 \equiv F_1(\text{steady state}) = F_2(0) = -\rho[x(1 - f_T + nf_T) - y(1 - f_D + \gamma f_D)]$$

The quotient of $\Delta_1/\Delta_2$ is given by

$$\Delta_1/\Delta_2 = (\rho - 0.75)/\rho$$

and therefore

$$\rho = 0.75/(1 - \Delta_1/\Delta_2)$$

Note that $\rho$ does not depend on the specific fluorescence intensity of the kinetic intermediates. In the case of the experiment discussed, $\Delta_1/\Delta_2 = -1/2$; therefore, $\rho = 0.5$; that is, 50% of the S-1 is in the states M·D·$P_i$ and AM·D·$P_i$ at steady state.

**Registry No.** ATPase, 9000-83-3; phosphate, 14265-44-2.

References

Adelstein, R. S., & Eisenberg, E. (1980) *Annu. Rev. Biochem. 49*, 921–956.

Barany, M. (1967) in *The Contractile Process*, pp 197–216, Little, Brown and Co., Boston, MA.

Brenner, B., Schoenberg, M., Chalovich, J. M., Greene, L. E., & Eisenberg, E. (1982) *Proc. Natl. Acad. Sci. U.S.A. 79*, 7288–7291.

Chock, S. P., Chock, P. B., & Eisenberg, E. (1979) *J. Biol. Chem. 254*, 3236–3243.

Eisenberg, E., & Kielley, W. W. (1972) *Cold Spring Harbor Symp. Quant. Biol. 37*, 145–152.

Eisenberg, E., & Kielley, W. W. (1974) *J. Biol. Chem. 249*, 4742–4748.

Eisenberg, E., & Greene, L. E. (1980) *Annu. Rev. Physiol. 42*, 293–309.

Eisenberg, E., Zobel, C. R., & Moos, C. (1968) *Biochemistry 7*, 3186–3194.

Eisenberg, E., Hill, T. L., & Chen, Y. (1980) *Biophys. J. 29*, 195–227.

Greene, L. E., Sellers, J. R., Eisenberg, E., & Adelstein, R. S. (1983) *Biochemistry 22*, 530–535.

Huxley, A. F. (1957) *Prog. Biophys. Biophys. Chem. 7*, 255–313.

Johnson, K. A., & Taylor, E. W. (1978) *Biochemistry 17*, 3432–3442.

Kielley, W. W., & Harrington, W. F. (1960) *Biochim. Biophys. Acta 41*, 401–421.

Lymm, R. W., & Taylor, E. W. (1971) *Biochemistry 10*, 4617–4624.

Marsh, D. J., Stein, L. A., Eisenberg, E., & Lowey, S. (1982) *Biochemistry 21*, 1925–1928.

Marston, S. B. (1978) *FEBS Lett. 92*, 147–151.

Marston, S. B., & Taylor, E. W. (1980) *J. Mol. Biol. 139*, 573–600.

Mornet, D., Bertrand, R., Pantel, P., Audemard, E., & Kassab, R. (1981) *Nature (London) 292*, 301–306.

Sellers, J. R., Eisenberg, E., & Adelstein, R. S. (1982) *J. Biol. Chem. 257*, 13880–13883.

Sleep, J. A., & Boyer, P. D. (1978) *Biochemistry 17*, 5417–5422.

Spudich, J. A., & Watt, S. (1971) *J. Biol. Chem. 246*, 4866–4871.

Stein, L. A., Schwarz, R. P., Chock, P. B., & Eisenberg, E. (1979) *Biochemistry 18*, 3895–3909.

Stein, L. A., Chock, P. B., & Eisenberg, E. (1981) *Proc. Natl. Acad. Sci. U.S.A. 78*, 1346–1350.

Stein, L. A., Chock, P. B., & Eisenberg, E. (1982) *Biophys. J. 37*, 264a.

Stein, L. A., Greene, L. E., Chock, P. B., & Eisenberg, E. (1983) *Biophys. J. 41*, 301a.

Wagner, R. D., & Weeds, A. L. (1979) *Biochemistry 18*, 2260–2266.

Weeds, A. G., & Taylor, R. S. (1975) *Nature (London) 257*, 54–56.